

Numerical Simulation of Conjugate Porous Channels at the Upper Scale of a Two Scale Hierarchical Media

V. S. Travkin, K. Hu, I. Catton

Department of Mechanical and Aerospace Engineering
University of California, Los Angeles
Los Angeles, CA 90095

ABSTRACT

The objective of this work is to describe the numerical methods used to solve a mathematical model that predicts laminar and turbulent flow and heat transfer for plane two-dimensional channels. The problem is treated in a two steps. The first step is to derive partial differential equations for momentum and energy conservation in the fluid and solid phases (two temperatures) in the channel derived from volume averaging theory (VAT) for heterogeneous media with a continuous incremental changing of the porosity and specific surface area. The second step is to solve the set of equations using a numerical method so that turbulent flow and heat transfer in porous media can be simulated. The channel investigated is assumed to be filled with a regular arrangements of discrete arbitrary obstacles. The transport equations for the REV are based on VAT and are given in this paper. These equations allow investigation of virtually an unlimited variety of morphological structures in a channel. The obstacles in

the channel are assumed to be symmetrically shaped and regularly arranged. The flow in the channel is steady state, fully developed, laminar or turbulent and incompressible. After constructing some closure models for the above equations, numerical solutions of the resulting model equations for turbulent flow and heat transfer in a channel filled with spherical beads or square tube banks are obtained and found to compare well with experimental results.

Nomenclature

- b - mean turbulent fluctuation energy = $\frac{1}{2}\overline{u_i^2}$ [m^2/s^2]
- c_d - mean drag resistance coefficient in the REV [-]
- c_p - specific heat [$J/(kg \cdot K)$]
- C_1 - constant coefficient in Kolmogorov turbulent exchange coefficient correlation [-]
- d_h - hydraulic dynameter, [m]
- d_p - side length or diameter of the unit [m]

dS	- interphase differential area in porous medium [m^2]
∂S_w	- internal surface in the REV [m^2]
f	- friction factor
\tilde{f}	- averaged over $\Delta\Omega_f$ value f
$\langle f \rangle_f$	- value f , averaged over $\Delta\Omega_f$ in a REV
\hat{f}	- value f morpho-fluctuation in a Ω_f
H	- width of the channel [m]
h	- half-width of the channel [m]
k	- thermal conductivity [$W/(mK)$]
k_{e1}	- key variable
K_m	- averaged turbulent eddy viscosity [m^2/s]
K_{sT}	- effective thermal conductivity of solid phase [$W/(mK)$]
K_T	- turbulent eddy thermal conductivity [$W/(mK)$]
l	- turbulence mixing length [m]
m	- porosity [-]
$\langle m \rangle$	- averaged porosity [-]
P	- pitch [m]
p	- pressure [Pa]
Re_{por}	- Reynolds number of pore hydraulic diameter [-]
S_w	- specific surface of a porous medium $\partial S_w/\Delta\Omega$ [$1/m$]
S_{wp}	- $= S_{\perp}/\Delta\Omega$ [$1/m$]
S_{\perp}	- cross flow projected area of obstacles [m^2]
T	- temperature [K]
T_s	- averaged solid phase temperature
u, w	- velocity in x,z-direction [m/s]
V	- volume [m^3]
x	- flow direction [m]
z	- direction perpendicular to the wall

Subscripts

f	- fluid phase, or, Fanning
i	- component of turbulent vector variable
L	- laminar
s	- solid phase
T	- turbulent

Superscripts

\sim	- value in fluid phase averaged over the REV
$-$	- mean turbulent quantity
s	- iteration number

Greek letters

$\tilde{\alpha}_T$	- averaged heat transfer coefficient over ∂S_w [$W/(m^2K)$]
$\Delta\Omega$	- representative elementary volume (REV) [m^3]
$\Delta\Omega_f$	- pore volume in a REV [m_3]
$\Delta\Omega_s$	- solid phase volume in a REV [m_3]
σ_b	- turbulent coefficient exchange ratio \tilde{K}_m/K_b [-]
σ_T	- turbulent coefficient exchange ratio \tilde{K}_m/\tilde{K}_T [-]
ν	- kinematic viscosity [m^2/s]
ρ	- density [kg/m^3]
τ	- turbulent friction stress tensor [N/m^2] = $-\rho\overline{u'w'}$
τ_w	- wall shear stress [N/m^2]

1 Introduction

Interest in turbulent flow and heat transfer in porous media is motivated by a wide range of thermal engineering applications ranging from geothermal systems, oil extraction, solid matrix heat exchangers, ground water pollution, thermal insulation to the storage of nuclear wastes. Transport phenomena in fluid-saturated porous media has been the topic of numerous studies published in the literature in recent years. For example, laminar flow and heat transfer through a porous flat channel with isothermal boundaries were considered in the research of Kaviany (1985). The solution of

the equations used by Kaviany, close to those used by Vafai and Tien (1981), showed the influence a porous medium morphology parameter $\gamma = (h^2 m_0 / K)^{1/2}$ on the results. Nowadays transport phenomena in porous media can be investigated in detail because of the progress in computer performance and numerical methods. The number of publications devoted to the development of numerical methods for solving problems of transport in porous media increases every year. Travkin and Catton (1992) presented a new model of turbulent flow and of two temperature heat transfer in a 2-D channel with highly porous medium. Huang and Vafai (1994) presented a detailed numerical investigation (vorticity - stream function method) of forced convection enhancement in a parallel plate channel with a porous block obstacle on one side of the wall. Travkin et al. (1998) investigated the channel flow characteristics as the channel flow porosity approaches unity through numerical simulation.

The main purpose of the present paper is to discuss the state-of-the art in modeling of flow and heat transfer in porous media using modern applied and computational mathematics. To accomplish this, detailed numerical simulation scheme as well as the mathematical model for flow and heat transfer in porous media will be discussed in this paper. The physical problem chosen is flow of a Newtonian fluid through a channel assumed to be roughened or filled with a regular arrangement of discrete arbitrary obstacles. The representative elementary volume (REV) in the porous layer is defined as the volume contained in a plane rectangular region parallel to the subsurface or a disk whose horizontal dimensions are far greater than characteristic dimensions of the obstacles. The obstacle elements of the channel are assumed to be symmetrically shaped and regularly arranged, and the flow in the chan-

nel is steady, fully developed, turbulent and incompressible. This approach was used in previous studies and demonstrated encouraging results for a channel with highly rough surfaces (Travkin and Catton, 1992, 1995, 1999).

This paper is organized as follows. The basic equations governing the flow and heat transport in porous media are presented in Section 2. Finite difference method based on Samarskii (1989) for solving those governing equations are discussed in Section 3 and Section 4 shows some numerical simulation cases. Finally, some concluding remarks can be found in Section 5.

2 Mathematical Models For Flow in a Channel Filled With Porous Media

The momentum equation for incompressible turbulent 1D flow in a channel filled with a porous media based on $K - \varepsilon$ modeling was developed in previous works (see Travkin and Catton (1992, 1995) or Gratton et al. (1996)).

A one dimensional flow model for fully developed steady state conditions that accounts for the morphological structure of the rough wall layer when there is no penetration through the elemental specific surface area ∂S_w , an impermeable interface, and a statistically homogeneous stream after closure specified by regularity of porous medium elements yields the form

$$\begin{aligned} & \frac{\partial}{\partial z} \left(\langle m(z) \rangle \tilde{K}_m(z) \frac{\partial \tilde{u}(z)}{\partial z} \right) \quad (1) \\ & = \frac{1}{2} c_d(z) S_w(z) \tilde{u}^2 + \frac{1}{\rho_f} \frac{d \langle \bar{p} \rangle_f}{dx}. \end{aligned}$$

Note that the above equation limits correctly to open channel flow when $\langle m \rangle$ approaches unity and S_w approaches zero. In the central part of the channel with a rough layer, when in the out of the rough layer, the porosity $\langle m \rangle = 1$ and the specific surface area $\partial S_w = 0$.

This simplifies the above equation to

$$\frac{\partial}{\partial z} \left(\langle m(z) \rangle \left(\tilde{K}_m + \nu \right) \frac{\partial \tilde{u}(z)}{\partial z} \right) = \frac{1}{\rho_f} \frac{\partial \left(\langle m(z) \rangle \tilde{p} \right)}{\partial x} \quad (2) \quad = \frac{\partial}{\partial z} \left(\langle 1 - m(z) \rangle K_{sT}(z) \frac{\partial T_s(x, z)}{\partial z} \right) \quad (6)$$

$$= \tilde{\alpha}_T(z) S_w(z) \left(T_s(x, z) - \tilde{T}(x, z) \right),$$

Following the theoretical assumptions of Monin and Yaglom (1975) and of Menzhulin (1970) that most of the interaction kinetic energy is transferred to the turbulent kinetic energy, Travkin and Catton (1992) suggested an equation for the mean turbulent fluctuation energy $b(z)$ of the form

$$\tilde{K}_m(z) \left(\frac{\partial \tilde{u}}{\partial z} \right)^2 + \frac{d}{dz} \left(\left(\frac{\tilde{K}_m}{\sigma_b} + \nu \right) \frac{db(z)}{dz} \right) + 2\nu \left(\frac{db^{1/2}(z)}{dz} \right)^2 + \frac{f_1(c_d) S_w(z)}{\langle m \rangle} \tilde{u}^3 \quad (3)$$

$$- \frac{g}{T_a \sigma_T} \left[\tilde{K}_m \frac{\partial \tilde{T}}{\partial z} \right] = C_1 \frac{b^2(z)}{\tilde{K}_m},$$

where the mean eddy viscosity $\tilde{K}_m(z)$ is given by

$$\tilde{K}_m(z) = C_1^{1/4} l(z) b^{1/2}(z), \quad (4)$$

and $l(z)$ is a turbulent scale function defined by the porous medium structure. The fourth term on the left hand side is the contribution of form drag.

Similarly, the energy equation for the fluid phase within the wall porous structure is

$$c_{pf} \rho_f \langle m \rangle \tilde{u}(z) \frac{\partial \tilde{T}(x, z)}{\partial x} \quad (5)$$

$$= \frac{\partial}{\partial z} \left(\langle m(z) \rangle \tilde{K}_T(z) \frac{\partial \tilde{T}(x, z)}{\partial z} \right)$$

$$+ \tilde{\alpha}_T(z) S_w(z) \left(T_s(x, z) - \tilde{T}(x, z) \right),$$

and in the solid phase of the wall layer, the corresponding equation for the solid phase volume averaged temperature is

with $(x, z) \in \Delta\Omega_s$, $P_{rT} = 1$ and $\tilde{K}_T = \tilde{K}_m c_{pf} \rho_f + k_f$. In the limit as the rough layer becomes more and more open or as the thickness of the rough layer becomes less and less, the porosity of the rough layer tends to unity leading to $\langle m \rangle = 1$ and $S_w = 0$. This will simplify the transport equations. The simplified transport equations are exactly the same as the momentum and heat transport equations of clear channel.

The boundary conditions for these equations are

$$z = 0 : \tilde{u} = 0, \frac{\partial b}{\partial z} = 0, \tilde{K}_m = \nu, K_{mk} = k_f,$$

$$Q_0 = -K_{sT} \frac{\partial T_s}{\partial z}, \quad \text{also} \quad Q_0 = -\tilde{K}_T \frac{\partial \tilde{T}}{\partial z} \quad (7)$$

$$z = h : \frac{\partial \tilde{u}}{\partial z} = 0, \frac{\partial b}{\partial z} = 0, \frac{\partial \tilde{T}}{\partial z} = 0, \frac{\partial T_s}{\partial z} = 0$$

In the laminar regime, the governing equations and closure models are much simpler. The physical process is governed by three equations instead of the five equations needed for the turbulent regime. The coefficient of viscosity and conductivity in laminar VAT equations are constants, and the porosity and specific surface function are functions of morphological models of the porous structure. This mathematical statement is used in cases where overall morphology and momentum transport conditions determine a low transport rates.

3 Numerical Scheme

3.1 Numerical scheme for momentum and kinetic energy balance equations

It is assumed that pressure gradient is a constant for flow across regular arranged porous

channel. The momentum equation (1) for the turbulent regime can be written in the form

$$\begin{aligned} & \frac{\partial}{\partial z} \left(k1_u \left(z, b, \tilde{u}, \tilde{T}, T_s \right) \frac{\partial \tilde{u}(z)}{\partial z} \right) \quad (8) \\ & = S1_u \left(z, \tilde{u} \right) + S2_u. \end{aligned}$$

When this equation is approximated by a three point stencil (z_{i-1}, z_i, z_{i+1}), the result is a second order difference equation with variable coefficients of the form

$$\begin{aligned} & A_{ju}^s \tilde{u}_{j-1}^{s+1} - C_{ju}^s \tilde{u}_j^{s+1} + B_{ju}^s \tilde{u}_{j+1}^{s+1} \quad (9) \\ & = -F_{ju}^{s+1}, \quad j = 1, 2, \dots, N-1 \end{aligned}$$

The momentum equation (8) is next discretized to yield

$$\begin{aligned} & \left(\frac{\varkappa_{01} a_j}{h_j \tilde{h}_j} \right) \tilde{u}_{j-1}^{s+1} \\ & - \left(\frac{\varkappa_{01} a_j}{h_j \tilde{h}_j} + \frac{\varkappa_{01} a_{j+1}}{h_{j+1} \tilde{h}_j} + \frac{1}{2} c_{d_j} S_{w_j} \tilde{u}_j \right) \tilde{u}_j^{s+1} \\ & + \left(\frac{\varkappa_{01} a_{j+1}}{h_{j+1} \tilde{h}_j} \right) \tilde{u}_{j+1}^{s+1} = -F_{ju}^s, \quad (10) \end{aligned}$$

where

$$\begin{aligned} A_{ju}^s &= \frac{\varkappa_{01} a_j^s}{h_j \tilde{h}_j} \\ B_{ju}^s &= \frac{\varkappa_{01} a_{j+1}^s}{h_{j+1} \tilde{h}_j} \\ C_{ju}^s &= \frac{\varkappa_{01} a_j^s}{h_j \tilde{h}_j} + \frac{\varkappa_{01} a_{j+1}^s}{h_{j+1} \tilde{h}_j} + \frac{1}{2} c_{d_j} S_{w_j} \tilde{u}_j^s \\ F_{ju}^s &= -\frac{k_{e1} \langle m_j \rangle}{\varrho_f} \left(\frac{d\tilde{p}}{dx} \right)^s = F_{ju}^{s+1} \\ \tilde{h}_j &= \frac{h_j + h_{j+1}}{2} \\ a_{j+1} &= k1_{j+0.5} = \frac{k1_j + k1_{j+1}}{2} \\ a_j &= k1_{j-0.5} = \frac{k1_j + k1_{j-1}}{2} \\ k1_j &= k1_{uj} = \langle m_j \rangle \tilde{K}_{mj}^s \\ \tilde{K}_m &= \nu_T + \nu = C_1^{1/4} l(z) b^{1/2}(z) + \nu. \end{aligned}$$

The equation for turbulent kinetic energy can be transformed in the same way.

3.2 Numerical scheme for energy equation in fluid phase

The energy equation (5) in the fluid phase has the simplified form

$$\begin{aligned} & k0 \left(z, \tilde{u} \right) \frac{\partial \tilde{T}(x, z)}{\partial x} \quad (11) \\ & = \frac{\partial}{\partial z} \left[k1_T \left(z, \tilde{u}, \tilde{T} \right) \frac{\partial \tilde{T}(x, z)}{\partial z} \right] \\ & + S1_T \left(z, \tilde{T}, T_s \right). \end{aligned}$$

The discretized version of the above equation can be written as

$$k0_j \frac{\left(\tilde{T}_{i,j} - \tilde{T}_{i-1,j} \right)}{h_i} = \Lambda_2 \tilde{T}_{i,j} + S1_{Tj} \quad (12)$$

where the operator $\Lambda_2 \tilde{\tilde{T}}_{i,j}$ is given by

$$\begin{aligned} \Lambda_2 \tilde{\tilde{T}}_{i,j} &= \frac{\partial}{\partial z} \left[k1_T (z, \tilde{u}, \tilde{T}) \frac{\partial \tilde{\tilde{T}}(x, z)}{\partial z} \right] \\ &= \left(\frac{\varkappa_{01} a_j}{h_j \tilde{h}_j} \right) \tilde{\tilde{T}}_{i,j-1}^{s+1} + \left(\frac{\varkappa_{01} a_{j+1}}{h_{j+1}} \right) \tilde{\tilde{T}}_{i,j+1}^{s+1} \\ &\quad - \left(\frac{\varkappa_{01} a_j}{h_j \tilde{h}_j} + \frac{\varkappa_{01} a_{j+1}}{h_{j+1} \tilde{h}_j} \right) \tilde{\tilde{T}}_{i,j}^{s+1}. \end{aligned} \quad (13)$$

The energy equation can be rearranged to

$$\begin{aligned} &- \left(c_{pf} \varrho_f \langle m \rangle \tilde{u} \right)_j \frac{\tilde{\tilde{T}}_{i-1,j}}{h_i} \\ &= \left(\frac{\varkappa_{01} a_j}{h_j} \right) \tilde{\tilde{T}}_{i,j-1} \\ &\quad - \left(\frac{\varkappa_{01} a_j}{h_j \tilde{h}_j} + \frac{\varkappa_{01} a_{j+1}}{h_{j+1} \tilde{h}_j} \right) \tilde{\tilde{T}}_{i,j} \\ &\quad - \left(\left(c_{pf} \varrho_f \langle m \rangle \tilde{u} \right)_j \frac{1}{h_i} + \tilde{\alpha}_{T_j}^s S_{w_j} \right) \tilde{\tilde{T}}_{i,j} \\ &\quad + \left(\frac{\varkappa_{01} a_{j+1}}{h_{j+1} \tilde{h}_j} \right) \tilde{\tilde{T}}_{i,j+1} + \tilde{\alpha}_{T_j}^s S_{w_j} T_{s,i,j}. \end{aligned} \quad (14)$$

allowing it to be written in the form

$$\begin{aligned} &A_{jT}^s \tilde{\tilde{T}}_{i,j-1}^{s+1} - C_{jT}^s \tilde{\tilde{T}}_{i,j}^{s+1} \\ &\quad + B_{jT}^s \tilde{\tilde{T}}_{i,j+1}^{s+1} + C_{jTs}^s T_{s,j}^{s+1} \\ &= -F_{jT}^s \end{aligned} \quad (15)$$

where

$$\begin{aligned} A_{jT}^s &= \frac{\varkappa_{01} a_j}{h_j \tilde{h}_j} \\ B_{jT}^s &= \frac{\varkappa_{01} a_{j+1}}{h_{j+1} \tilde{h}_j} \\ C_{jT}^s &= \frac{\varkappa_{01} a_j}{h_j \tilde{h}_j} + \frac{\varkappa_{01} a_{j+1}}{h_{j+1} \tilde{h}_j} \\ &\quad + \left(c_{pf} \varrho_f \langle m \rangle \tilde{u} \right)_j \frac{1}{h_i} + \tilde{\alpha}_{T_j}^s S_{w_j} \\ C_{jTs}^s &= \tilde{\alpha}_{T_j}^s S_{w_j} \\ F_{jT}^s &= \left(c_{pf} \varrho_f \langle m \rangle \tilde{u} \right)_j \frac{\tilde{\tilde{T}}_{i-1,j}^s}{h_i} \\ \tilde{h}_j &= \frac{h_j + h_{j+1}}{2} \\ a_{j+1} &= k1_{j+0.5} = \frac{k1_j + k1_{j+1}}{2} \\ a_j &= k1_{j-0.5} = \frac{k1_j + k1_{j-1}}{2} \\ k1_j &= k1_{T_j} = \langle m_j \rangle \tilde{K}_{T_j}^s \\ \tilde{K}_T &= K_T + k_f. \end{aligned}$$

The boundary conditions for the fluid phase energy equation are the following:

At the channel inlet, $x = 0$

$$T_s|_{x=0} = \tilde{\tilde{T}}|_{x=0} = T_{in} = const \quad (16)$$

At the top of the channel, $z = h$

$$\begin{aligned} \frac{\partial \tilde{\tilde{T}}(x, z)}{\partial z} \Big|_{z=h} &= 0 \\ \frac{\partial T_s(x, z)}{\partial z} \Big|_{z=h} &= 0 \end{aligned} \quad (17)$$

At the bottom of the channel, $z = 0$

$$\begin{aligned} &\langle m(z) \rangle \tilde{K}_T(z) \frac{\partial \tilde{\tilde{T}}(x, z)}{\partial z} \\ &= \tilde{\alpha}_T(z) S_{\perp}(z) \left[T_s(x, z) - \tilde{\tilde{T}}(x, z) \right] \\ &\quad - \langle m \rangle Q_{out}. \end{aligned} \quad (18)$$

3.3 Numerical scheme for energy equation in solid phase

The energy equation (6) in the solid phase is transformed to

$$\begin{aligned} & \frac{\partial}{\partial x} \left[k1_{Ts} \frac{\partial T_s(x, z)}{\partial x} \right] + \frac{\partial}{\partial z} \left[k1_{Ts} \frac{\partial T_s(x, z)}{\partial z} \right] \\ & = S2_T \left(z, \tilde{T}, T_s \right). \end{aligned} \quad (19)$$

The difference form of the above equation can be written as

$$\Lambda_1 T_{si,j} + \Lambda_2 T_{si,j} = S2_{Tj}, \quad (20)$$

where

$$\begin{aligned} \Lambda_1 T_{si,j} &= \frac{\partial}{\partial x} k1_{Ts} \left[\frac{\partial T_s(x, z)}{\partial x} \right] \\ &= \left(\frac{\varkappa_{01} a_j}{h_i \tilde{h}_i} \right) T_{si-1,j} \\ &\quad + \left(\frac{\varkappa_{01} a_j}{h_{i+1} \tilde{h}_i} \right) T_{si+1,j} \\ &\quad - \left(\frac{\varkappa_{01} a_j}{h_i \tilde{h}_i} + \frac{\varkappa_{01} a_j}{h_{i+1} \tilde{h}_i} \right) T_{si,j} \end{aligned} \quad (21)$$

$$\begin{aligned} \Lambda_2 \tilde{T}_{i,j} &= \frac{\partial}{\partial z} \left[k1_{Ts}(z) \frac{\partial T_s(x, z)}{\partial z} \right] \\ &= \left(\frac{\varkappa_{01} a_j}{h_j \tilde{h}_j} \right) T_{si,j-1} \\ &\quad + \left(\frac{\varkappa_{01} a_{j+1}}{h_{j+1} \tilde{h}_j} \right) T_{si,j+1} \\ &\quad - \left(\frac{\varkappa_{01} a_j}{h_j \tilde{h}_j} + \frac{\varkappa_{01} a_{j+1}}{h_{j+1} \tilde{h}_j} \right) T_{si,j} \end{aligned} \quad (22)$$

and can be put in the form

$$\begin{aligned} & A_{jTs}^s T_{si,j-1}^{s+1} - C_{jTs}^{s+1} T_{si,j}^{s+1} \\ & + B_{jTs}^s T_{si,j+1}^{s+1} + C_{jTFs}^s \tilde{T}_{ij}^{s+1} \\ & = -F_{jTs}^s \end{aligned} \quad (23)$$

where

$$\begin{aligned} A_{jTs}^s &= \frac{\varkappa_{01} a_j}{h_j \tilde{h}_j} \\ B_{jTs}^s &= \frac{\varkappa_{01} a_{j+1}}{h_{j+1} \tilde{h}_j} \\ C_{jTs}^s &= \frac{\varkappa_{01} a_j}{h_j \tilde{h}_j} + \frac{\varkappa_{01} a_{j+1}}{h_{j+1} \tilde{h}_j} \\ &\quad + \frac{\varkappa_{01} a_j}{h_i \tilde{h}_i} + \frac{\varkappa_{01} a_{j+1}}{h_{i+1} \tilde{h}_i} + \tilde{\alpha}_{Tj} S_{w_j} \\ C_{jTFs}^s &= \tilde{\alpha}_{Tj}^s S_{w_j} \\ F_{jTs}^s &= \left(1 - \langle m \rangle_j \right) \tilde{S}_{Tj}^s \\ &\quad + \frac{a_j}{h_i \tilde{h}_i} T_{si-1,j} + \frac{a_{j+1}}{h_{i+1} \tilde{h}_i} T_{si+1,j} \\ \tilde{h}_i &= \frac{h_i + h_{i+1}}{2} \\ \tilde{h}_j &= \frac{h_j + h_{j+1}}{2} \\ a_{j+1} &= k1_{j+0.5} = \frac{k1_j + k1_{j+1}}{2} \\ a_j &= k1_{j-0.5} = \frac{k1_j + k1_{j-1}}{2} \\ k1_j &= k1_{Ts_j} = (1 - \langle m_j \rangle) \tilde{K}_{sTj}^s \\ \tilde{K}_{sT} &= k_s. \end{aligned}$$

3.4 Equations solving procedures

When solving the above set of equations (9),(15) and(23) the momentum equation and turbulent kinetic energy equation need to be solved first. The exact solution of equation (9) for \tilde{u}_j follows from

$$\tilde{u}_N = \frac{\nu_2 + \varkappa_2 \beta_N}{1 - \varkappa_2 \alpha_N} \quad (24)$$

and

$$\tilde{u}_j = \alpha_{j+1} \tilde{u}_{j+1} + \beta_{j+1} \quad 0 \leq j \leq N-1 \quad (25)$$

where

$$\alpha_1 = \varkappa_1 \quad \beta_1 = \nu_1 \quad (26)$$

and

$$\alpha_{j+1} = \frac{B_j}{C_j - \alpha_j A_j}, \quad 1 \leq j \leq N-1 \quad (27)$$

$$\beta_{j+1} = \frac{A_j \beta_j + F_j}{C_j - \alpha_j A_j}, \quad 1 \leq j \leq N-1 \quad (28)$$

After solving the momentum equation and kinetic energy equation, the energy equations can be solved. Since the heat transfer problem for flow in porous media is a conjugate problem, the fluid phase and solid phase heat transport equations must be solved simultaneously instead of solving fluid phase heat transport equation only. To aid in the solution procedure, Eq. (15) and Eq. (23) are combined and written in the form

$$\begin{aligned} \overset{\circ}{A}_j \bar{Y}_{j+1} - \overset{\circ}{B}_j \bar{Y}_j + \overset{\circ}{C}_j \bar{Y}_{j-1} &= -\bar{F}_j \quad 1 \leq j \leq N-1. \end{aligned} \quad (29)$$

where

$$\begin{aligned} \bar{Y}_j &= \begin{bmatrix} \tilde{T}_{ij}^{s+1} \\ T_{sij}^{s+1} \end{bmatrix}, & (30) \\ \overset{\circ}{A}_j &= \begin{bmatrix} B_{jT}(\tilde{T}) & 0 \\ 0 & B_{jT}(T_s) \end{bmatrix}, \\ \overset{\circ}{B}_j &= \begin{bmatrix} C_{jT}(\tilde{T}) & C_{jTS} \\ C_{jTF} & C_{jT}(T_s) \end{bmatrix}, \\ \overset{\circ}{C}_j &= \begin{bmatrix} A_{jT}(\tilde{T}) & 0 \\ 0 & A_{jT}(T_s) \end{bmatrix}, \\ \bar{F}_j &= \begin{bmatrix} F_{jT}(\tilde{T}) \\ F_{jT}(T_s) \end{bmatrix} \quad 1 \leq j \leq N-1 \end{aligned}$$

The solution of equation (29) can be written in the form

$$\bar{Y}_{j-1} = X_j \bar{Y}_j + \bar{Z}_j, \quad j = N, N-1, \dots, 2, 1. \quad (31)$$

The calculations needed to obtain grid values of $\tilde{T}_{i,j}^{s+1}$ and T_{sij}^{s+1} are

$$\begin{aligned} X_1 &= B_0^{-1} A_0, \quad \bar{Z}_1 = B_0^{-1} \bar{F}_0 \\ X_{j+1} &= \left(\overset{\circ}{B}_j - \overset{\circ}{C}_j \cdot X_j \right)^{-1} \overset{\circ}{A}_j, \\ \bar{Z}_{j+1} &= \left(\overset{\circ}{B}_j - \overset{\circ}{C}_j \cdot X_j \right)^{-1} \left(\overset{\circ}{C}_j \bar{Z}_j + \bar{F}_j \right), \\ &1 \leq j \leq N-1 \end{aligned} \quad (32)$$

and

$$\begin{aligned} \bar{Y}_N &= (B_N - C_N X_N)^{-1} \cdot (C_N \bar{Z}_N + \bar{F}_N) \\ \bar{Y}_{j-1} &= X_j \bar{Y}_j + \bar{Z}_j, \quad j = N, N-1, \dots, 2, 1. \end{aligned} \quad (33)$$

Here B_j C_j , A_j , X_j B_0 , A_0 , B_N , C_N are matrices of 2nd order.

If written in matrix form, the lower boundary condition becomes

$$A_0 \bar{Y}_1 - B_0 \bar{Y}_0 = -\bar{F}_0 \quad (34)$$

where

$$\begin{aligned} A_0 &= \begin{bmatrix} \frac{\langle m \rangle_{0.5} \tilde{K}_{T,0.5}}{h_{j=1}} & 0 \\ 0 & \frac{(1 - \langle m \rangle_{0.5}) \tilde{K}_{ST,0.5}}{h_{j=1}} \end{bmatrix} \\ B_0 &= \begin{bmatrix} \frac{\langle m \rangle_{0.5} \tilde{K}_{T,0.5}}{h_{j=1}} - \tilde{\alpha}_{T,0} S_{\perp} & \tilde{\alpha}_{T,0} S_{\perp} \\ \tilde{\alpha}_{T,0} S_{\perp} & B_{022} \end{bmatrix} \\ B_{022} &= \frac{(1 - \langle m \rangle_{0.5}) \tilde{K}_{ST,0.5}}{h_{j=1}} - \tilde{\alpha}_{T,0} S_{\perp} \end{aligned} \quad (35)$$

$$\begin{aligned} \bar{Y}_1 &= \begin{bmatrix} \tilde{T}_{i,1}^2 \\ T_{S,1}^2 \end{bmatrix}, \quad \bar{Y}_0 = \begin{bmatrix} \tilde{T}_{i,0}^2 \\ T_{S,0}^2 \end{bmatrix}, \\ \bar{F}_0 &= \begin{bmatrix} \langle m \rangle_0 Q_{out} \\ (1 - \langle m \rangle_0) Q_{out} \end{bmatrix}. \end{aligned}$$

The upper boundary condition is written as

$$-B_N \bar{Y}_N + C_N \bar{Y}_{N-1} = -\bar{F}_N \quad (36)$$

where

$$B_N = \begin{bmatrix} 1 & 0 \\ 0 & 1 \end{bmatrix}, \quad \vec{Y}_N = \begin{bmatrix} \widetilde{T}_{i,N}^2 \\ \widetilde{T}_{S,N}^2 \end{bmatrix} \quad (37)$$

$$C_N = \begin{bmatrix} 1 & 0 \\ 0 & 1 \end{bmatrix}, \quad \vec{Y}_{N-1} = \begin{bmatrix} \widetilde{T}_{i,N-1}^2 \\ \widetilde{T}_{S,N-1}^2 \end{bmatrix}$$

$$\vec{F}_N = \begin{bmatrix} 0 \\ 0 \end{bmatrix}$$

So that

$$\begin{aligned} -\widetilde{T}_{i,N} + \widetilde{T}_{i,N-1} &= 0, \\ -\widetilde{T}_{S,N} + \widetilde{T}_{S,N-1} &= 0. \end{aligned} \quad (38)$$

Since temperature changes with both x and z , So iteration in x direction is also needed. Iterations are based on the equations given below,

$$k0_j \frac{(\widetilde{T}_{i+1,j} - \widetilde{T}_{i,j})}{h_i} = \Lambda_2 \widetilde{T}_{i,j} + S1_{Tj} \quad (39)$$

and

$$\begin{aligned} &\left(\frac{\varkappa_{01} a_j}{h_{i+1} \bar{h}_i} \right) T_{si+1,j} \quad (40) \\ &= \left(\frac{\varkappa_{01} a_j}{h_i \bar{h}_i} + \frac{\varkappa_{01} a_j}{h_{i+1} \bar{h}_i} \right) T_{si,j} - \left(\frac{\varkappa_{01} a_j}{h_i \bar{h}_i} \right) T_{si-1,j} \\ &\quad - \Lambda_2 T_{si,j} + S2_{Tj}. \end{aligned}$$

The final convergent solutions satisfied the following convrgent criteria for \widetilde{T} , T_s and \widetilde{u} , i.e.:

$$\left| \frac{\widetilde{T}^{s+1} - \widetilde{T}^s}{\widetilde{T}^s} \right| \leq 10^{-4}, \quad (41)$$

$$\left| \frac{T_s^{s+1} - T_s^s}{T_s^s} \right| \leq 10^{-4}, \quad (42)$$

and

$$\left| \frac{\widetilde{u}^{s+1} - \widetilde{u}^s}{\widetilde{u}^s} \right| \leq 10^{-4}. \quad (43)$$

4 Results and Discussion

In order to solve the model equations, many coefficient and mathematical models were developed. Watanabe (1989) proposed a drag model for flow through granular packed beds. The model can be applied over a wide range of the particle Reynolds number and can be used to derive various empirical formulas. All the coefficient models used and discussed in the present work are strictly for assumed (or admitted) porous medium morphological modes based on well described geometry. This approach shows that to model the morphology of a porous media, the coefficients in the equations as well as the equation form itself must be consistent. The integral terms in the equations can be dropped or transformed depending on the porous medium structure, flow and heat transfer regimes. Developed closures allow one to obtain exact analytical dependencies for simple porous medium morphologies.

In this section we present simulation results of VAT based transport models and closure models for flow in a channel with several typical morphology structures. For example , consider channel flow across round tube banks and channel flow across square tube banks. The morphology models used in the numerical simulation are shown in Fig.1 and Fig. 2. Fig. 1 shows the side view and the top view of a channel with height $2h$ filled with regularly arranged square cylinders with pitch P and side length d_p . Fig.2 shows the side view and the top view of a channel with height $2h$ filled with regularly arranged cylindrical tube banks with pitch P and diameter d_p . For flow across tube banks (square and cylindrical), the tubes are regularly arranged.

The grid sizes depend on the morphology model of porous medium. The grid size chosen for the models shown in Fig. 1 and Fig. 2 are $\Delta z = h/1000$ along z direction and

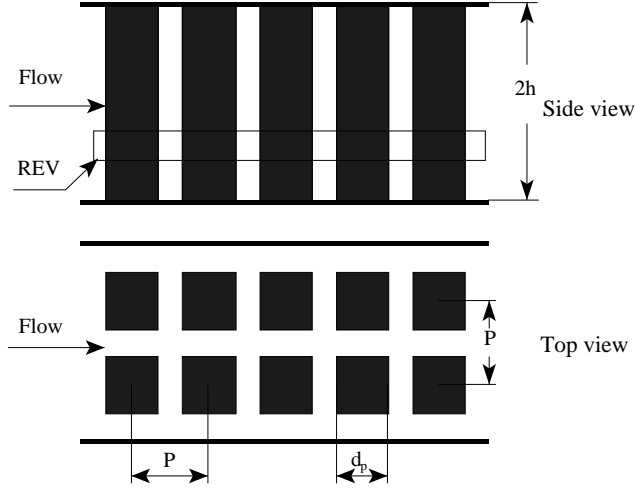


Figure 1: Channel flow across square tube banks

$\Delta x = h/1000$ along x direction.

4.1 Channel flow across square tube banks

In order to incorporate the morphology of a porous medium in the model equations, porosity m and specific surface S_w in each REV need to be specified. The REV porosity of the morphology model showed in Fig. 1 is

$$\langle m \rangle = \frac{\Delta \Omega_f}{\Delta \Omega} = 1 - \frac{d_p^2}{P^2}. \quad (44)$$

And REV specific surface is

$$S_w = \frac{\partial S_w}{\Delta \Omega} = \frac{4d_p \delta}{P^2 \delta} = \frac{4d_p}{P^2} \quad (45)$$

where δ is the REV height. So channel equivalent hydraulic diameter d_h is

$$d_h = \frac{4 \langle m \rangle}{S_w} = \frac{P^2 - d_p^2}{d_p}. \quad (46)$$

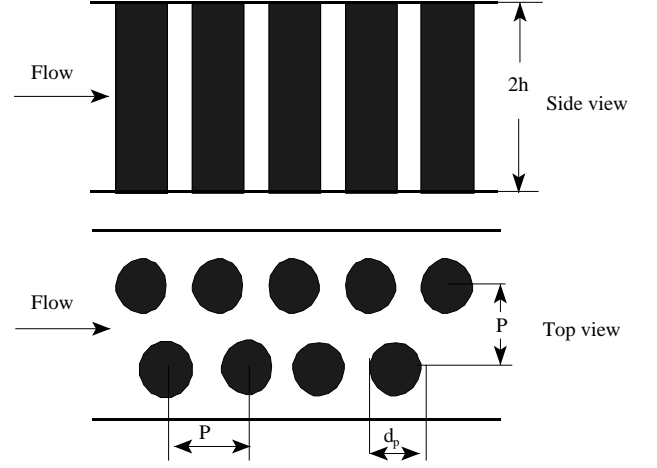


Figure 2: Flow across round tube banks

And channel porous Reynolds number is

$$Re_{por} = \frac{\tilde{u} d_h}{\nu} = \frac{\tilde{u} (P^2 - d_p^2)}{\nu d_p}. \quad (47)$$

The friction factor for flow across square tube banks was developed from Souto & Moyne (1997) through curve fitting. From this paper one can deduce that

$$\lg \frac{\Delta p'}{\Delta L'} = -1.0 \lg (Re_p) + 2.388 \quad (48)$$

where $\frac{\Delta p'}{\Delta L'}$ is defined in Souto & Moyne (1997) as

$$\begin{aligned} \frac{\Delta p'}{\Delta L'} &= \left(\frac{\Delta p}{\tilde{u}^2} \right) \left(\frac{\langle m \rangle \frac{6}{a_v}}{(1 - \langle m \rangle) \Delta L} \right) \quad (49) \\ &= \frac{\frac{3}{2} d_h}{\tilde{u}^2} \left(\frac{\Delta p}{\Delta L} \right) = 3f_f \end{aligned}$$

and

$$Re_p = \frac{\langle m \rangle \tilde{u} \frac{6}{a_v}}{(1 - \langle m \rangle) * \nu} = \frac{\tilde{u} (\frac{3}{2} d_h)}{\nu} = \frac{3}{2} Re_{por}. \quad (50)$$

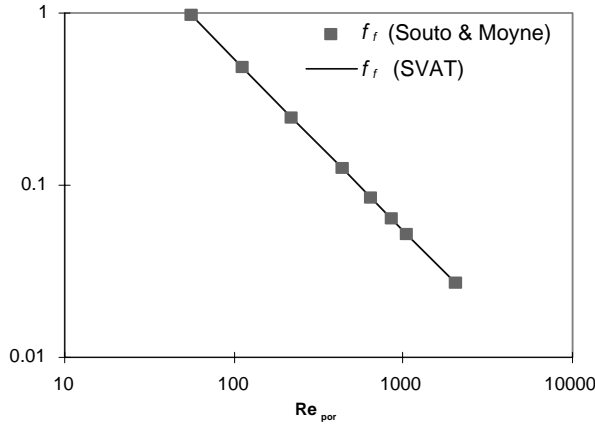


Figure 3: Comparison of the SVAT results and Souto and Moyne (1997)

where a_v is the ratio of the fluid solid surface to the volume of the particles. From the above three correlations, we can deduce that the Fanning friction factor is

$$f_f = \frac{1}{3} \frac{\Delta p'}{\Delta L'} = \frac{10^{2.388}}{3.0 * \frac{3}{2} Re_{por}} = \frac{54.3}{Re_{por}} \quad (51)$$

Compared with Souto & Moyne (1997), on Fig.3 the momentum resistance of SVAT model is in very close agreement.

Fig.4 is the velocity distribution when porosity approaches 0. When porosity becomes smaller and smaller, the form drag will play a more and more important role. At the same pressure gradient the larger the form drag, the smaller the velocity. From physical view point this is exactly what we expect.

4.2 Channel flow across round pin fins

To illustrate the validity of the present mathematical model and numerical scheme, another experiment conducted is to simulate air flow through staggered round pin fin channel. For

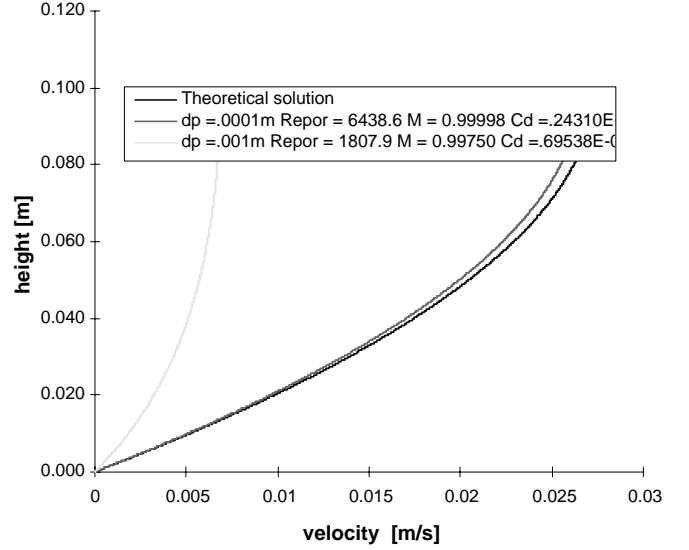


Figure 4: Channel average velocity of flow across square tube banks, $\langle m \rangle \rightarrow 1.0$

morphology model of pin fin channel the porosity and specific surface can be expressed as

$$\langle m \rangle = \frac{P^2 - \frac{1}{2}\pi d_p^2}{P^2} \quad (52)$$

$$S_w = \frac{2\pi d_p}{P^2} \quad (53)$$

The closures needed for $\tilde{\alpha}_T(z)$ and $c_d(z)$ which are used for momentum and energy transport across pin fin channel are derived from Zukauskas (1987). In order to compare numerical results with experimental results, the pin fin configuration chosen here is the same as that shown in Fig. 3 of Al-Jamal and Khashashneh (1998), that is $P = 28mm$ and $d_p = 12mm$. Fig. 5 shows a comparison of channel Nusselt number from present numerical results and the experimental results presented in Al-Jamal and Khashashneh (1998). The Nusselt number defined here, that defined by Al-Jamal and

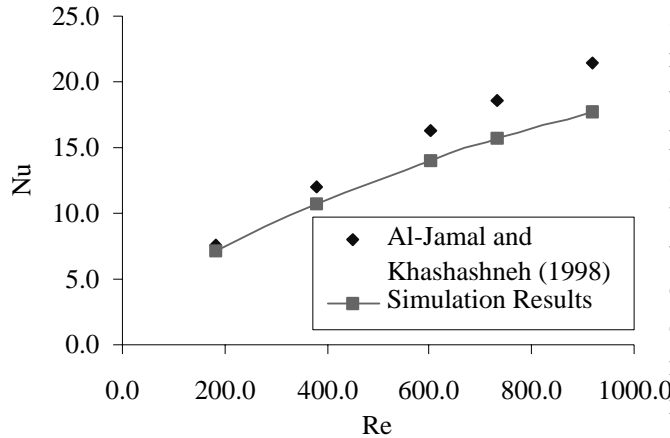


Figure 5: Pin-fins channel Nusselt number

Khashashneh (1998), is

$$Nu = \frac{Qd_p}{k_f S_{total} (T_w - T_f)} \quad (54)$$

where S_{total} is total heat transfer area in the channel, T_w is average wall temperature and T_f is average air temperature in the channel. From Fig.5 we can see that prediction is about 30% less than experimental results at the high Reynolds number, but they are comparable.

5 Summary and Discussion

The VAT, and SVAT, based equations are presented and tested for several cases. Under many circumstances this is dealt with by the author of the different equations choosing closure relations that match the data of interest to him. This does not help generate reliable analytical tools because the parameters needed to fully describe the media are missing. The result is wide variation in the predicted heat transfer or pressure drop for any given media. This study addresses some of these issues.

The main purpose of this study is to present a numerical scheme for the verification of closure

methodologies as well as comparison with available models for two dimensional channel flow in a porous medium. This was accomplished by first developing a numerical scheme for solving the model equations of flow in porous media presented by Travkin & Catton (1992,1995), and then applying the closure models to simulate the specific case of two dimensional flow through a porous medium. Through the application of the SVAT closure model to some general morphology models, such as pin fin channel flow, it is demonstrated that the transport model, closure scheme and numerical method are reasonable. The numerical results show that the model developed in this paper is applicable to the study of flow in channels with rough walls or in channels filled with regular porous matrix, and demonstrates that the simplest morphological properties of a porous layer such as porosity function and specific surface along with closure models naturally affects the transport fields in the channel.

Acknowledgment

This work was partly sponsored by the Department of Energy, Office of Basic Energy Sciences through the grant DE-FG03-89ER14033 A002. And partly sponsored by DARPA as part of the HERETIC program, grant # DAAD19-99-1-0157.

References

- Al-Jamal, K. and Khashashneh, H., 1998, Experimental investigation in heat transfer of triangular and pin fin arrays, *Heat and Mass Transfer*, Vol. 34, pp. 159-162.
- Gratton, L. J., Travkin, V. S. and Catton, I., 1996, The influence of morphology upon two-temperature statements for convective transport in porous medium, *Journal of Enhanced Heat Transfer*, Vol. 3, No. 2, pp. 129-145.
- Huang, P.C., and Vafai, K., 1994, Analysis of forced convection enhancement in a channel

using porous blocks, *J. of Thermophysics and Heat Transfer*, Vol. 8, No. 3, pp. 563-573.

Kaviany, M., 1985, Laminar flow through a porous channel bounded by isothermal parallel plates, *Int. J. Heat Mass Transfer*, Vol. 28, No. 4, pp. 851-858.

Menzhulin, G. V., 1970, The method of calculating the meteorological regimes in the vegetation cover, *Meteorology and Hydrology*, No. 2, pp. 92-99.

Monin, A. S. and Yaglom, A. M., 1975, *Statistical Fluid Mechanics*, Vol. 1, 2, MIT press, Cambridge, Massachusetts.

Samarskii A. A. 1989, *Numerical Methods for Grid Equations*, Birkhauser Verlag.

Souto, H. P. A. and Moyne, C. 1997, Dispersion in two dimensional periodic porous media, *Phys. Fluids*, Vol. 9, No. 8, pp. 2243-2263.

Travkin V. S. and Catton, I., 1992, Models of turbulent thermal diffusivity and transfer coefficients for a regular packed bed of spheres, *Procs., 28th National Heat Transfer Conference*, San Diego, CA, ASME, HTD-Vol. 193, pp. 15-23.

Travkin V. S. and Catton, I., 1995, A two temperature model for turbulent flow and heat transfer in a porous layer, *J. Fluids Engineering*, Vol. 117, pp. 181-188.

Travkin V. S. and Catton, I., 1998, Porous media transport descriptions - non-local, linear and non-linear against effective thermal / fluid properties, *Advances in Colloid and Interface Science*, Vol. 76-77, pp. 389-443.

Travkin, V. S., Catton, I. and Hu, K., 1998, Channel flow in porous media in the limit as porosity approaches unity, *Proceedings of the ASME Heat Transfer Division*, HTD-Vol. 361-1, pp. 277-284.

Travkin, V. S. and Catton, I., 1999, Turbulent flow and heat transfer modeling in a flat channel with regular highly rough walls, to be appeared in *International Fluid Mechanics Re-*

search.

Vafai, K., and Tien, C. L., 1981, Boundary and inertia effects on flow and heat transfer in porous media, *Int. J. Heat Mass Transfer*, Vol. 24, pp. 195-203.

Watanabe, H., 1989, Drag coefficient and voidage function on fluid flow through granular packed beds, *International Journal of Engineering Fluid Mechanics*, Vol. 2, No. 1, pp. 93-108.

Zukauskas, A., 1987, Convective heat transfer in cross flow, in "Handbook of Single-phase Convective Heat Transfer", edited by S. Kakac, R. K. Shah and W. Aung, *John Wiley & Sons*.